The properties of transparent conducting molybdenum-doped ZnO films grown by radio frequency magnetron sputtering*

Xiu Xian-Wu(修显武)[a)†] and Zhao Wen-Jing(赵文静)[b)]

[a)] *School of Physics and Electronics, Shandong Normal University, Jinan* 250014, *China*
[b)] *Jinan No.3 Vocational School, Jinan* 250001, *China*

(Received 1 November 2011; revised manuscript received 25 December 2011)

Transparent conducting molybdenum-doped zinc oxide films are prepared by radio frequency (RF) magnetron sputtering at ambient temperature. The MoO_3 content in the target varies from 0 to 5 wt%, and each film is polycrystalline with a hexagonal structure and a preferred orientation along the *c* axis. The resistivity first decreases and then increases with the increase in MoO_3 content. The lowest resistivity achieved is 9.2×10^{-4} $\Omega \cdot$cm, with a high Hall mobility of 30 $cm^2 \cdot V^{-1} \cdot s^{-1}$ and a carrier concentration of 2.3×10^{20} cm^{-3} at an MoO_3 content of 2 wt%. The average transmittance in the visible range is reduced from 91% to 80% with the increase in the MoO_3 content in the target.

Keywords: molybdenum oxide, zinc oxide, magnetron sputtering, transparent conducting oxides

PACS: 68.55.Ln, 73.61.Ga, 78.30.Fs **DOI:** 10.1088/1674-1056/21/6/066802

1. Introduction

The ever-increasing demand for transparent conducting oxides (TCOs) for use in flat panel displays, light-emitting diodes (LEDs), solar cells, photovoltaics, and architectural window applications, is the primary motivation for research on TCOs.[1−4] Among all TCOs, indium tin oxide (ITO) is most widely used because of its low resistivity, high transmittance, and high work function.[5] However, ITO usage has some problems because of the high cost of indium and its limited supply. In addition, the diffusion barrier characteristics and thermal stability of ITO pose a problem for transparent electrode in LEDs.[6,7] Recently, ZnO has been actively investigated as an alternate material to ITO because it is nontoxic, inexpensive, and abundant compared with ITO.[8,9] Moreover, ZnO is chemically stable in the hydrogen plasma that is commonly used in the fabrication of TFT-LCDs.[10] Al, Ga, In, Zr, B, and rare earth-doped ZnO films have all been studied. However, looking for new materials is still interesting and attractive.

In this paper, transparent conducting MZO films are prepared by radio frequency (RF) magnetron sputtering. The structural, electrical, and optical properties of these films are studied in detail, each as a function of the MoO_3 content in the target.

2. Experimental details

The MZO films were deposited on glass substrates in an MS350 RF (13.56 MHz) magnetron sputtering system. In order to optimize the MoO_3 content doped into ZnO, five sintered targets with a mixture of ZnO (purity of 99.99%) and MoO_3 (purity of 99.95%) were employed as source materials. The values of the MoO_3 content in the targets were 0, 1, 2, 3, and 5 wt%, respectively. The vacuum chamber was evacuated to 5×10^{-4} Pa before sputtering, and the sputtering was carried out in pure argon atmosphere. The distance between the target and the substrate was 2.5 cm. The RF power was maintained at 15 W and the pressure of the chamber was maintained at 0.6 Pa during deposition. Prior to deposition, the substrates were cleaned ultrasonically and degreased in acetone, and during sputtering, the substrates were not intentionally heated. The film thickness was 400 nm on average for all the samples.

The film thickness was measured using an XP-2^{TM} profilometer (Ambios Technology Company, USA). The structural properties were analysed with

*Project supported by the Science Foundation of the Education Commission of Shandong Province, China (Grant No. J10LA04).
†Corresponding author. E-mail: xwxiu@sdnu.edu.cn
© 2012 Chinese Physical Society and IOP Publishing Ltd

a Philips X' pert MRD diffractometer using a Cu Kα radiation source (λ = 1.542 Å, 1 Å = 0.1 nm). The morphology of the surface was observed by a DI NanoScope IIIa D3000 atomic force microscope (AFM). The electrical properties were measured with the four-point probe method, and Hall effect measurement was implemented using the Van der Pauw technique at a constant magnetic field of 0.5 T. The optical transmittance measurements were performed with a TU-1901 UV-VIS spectrophotometer.

3. Results and discussion

Figure 1 shows the XRD patterns of the MZO films each as a function of the MoO_3 content in the target. The insert in Fig. 1 shows a typical XRD pattern of the MZO film deposited at an MoO_3 content of 2 wt%. It can be seen that the MZO films grow without forming secondary phases and clusters such as MoO_3 and amorphous ZnO. All the films exhibit only the ZnO (002) peak, indicating that each film is polycrystalline with a hexagonal structure and a preferred orientation with the c axis perpendicular to the substrate. After studying the location of the diffraction peak carefully, we find that the ZnO (002) peak values (34.18°–34.33°) are lower than those of the standard ZnO crystal (34.45°), which is consistent with that reported in Ref. [11]. This is presumably due to the substitution of Mo^{2+}, which may come from the sputtering process. Because the ionic radius of Mo^{2+} is larger than that of Zn^{2+}, the length of the c axis is expected to be longer. Then the position of the ZnO (002) peak is expected to shift to a lower 2θ value. The crystalline quality of the MZO film can be evaluated by the intensity and the full width at half maximum (FWHM) of the ZnO (002) peak. The intensity of the peak significantly increases and the FWHM decreases as the MoO_3 content increases from 0 to 2 wt%, which suggests that the Mo doped in the ZnO film would stimulate grain growth and improve the crystallinity of the MZO film. A similar phenomenon was presented separately for the Tb-doped ZnO film[12] and Ga-doped ZnO film.[13] However, the intensity of the peak obviously decreases with the increase in the FWHM when the MoO_3 content increases further to 5 wt%, which indicates the deterioration of the crystallinity. The highly incorporated Mo^{6+} ions are not only at the substitutional sites, but also at the interstitial sites. When the MoO_3 content is higher, the number of Mo^{6+} ions in the interstitial sites increase with the MoO_3 content increasing, which leads to the deterioration of the crystallinity. The crystallite size evaluated by the Scherrer formula[14] as a function of MoO_3 content in the target is shown in Fig. 2. It can be seen that the crystallite size increases slightly as the MoO_3 content increases, reaching a highest value of 25 nm for the MoO_3 content of 2 wt%, and then decreases obviously with a further increase in MoO_3 content.

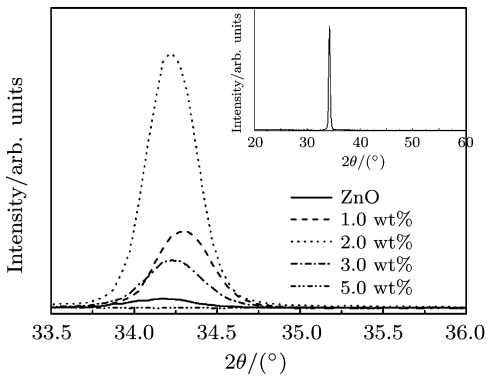


Fig. 1. The XRD patterns of MZO films, each as a function of the MoO_3 content in the target.

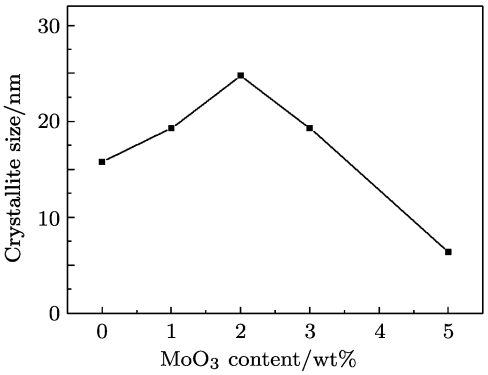


Fig. 2. The dependence of the crystallite size on the MoO_3 content in the target for the MZO film.

It is very important to investigate the surface morphology of the film because it can affect the properties of the device. Figure 3 shows an AFM image (1 μm × 1 μm) of the MZO film deposited with an MoO_3 content of 2 wt%. The film surface is dense and relatively smooth with a root-mean-square (RMS) surface roughness of approximately 4.5 nm. It can be seen that the film is composed of small grains with the sizes in a range of 35 nm–40 nm. Considering the crystallite size determined from the XRD data, the grains observed in the AFM are most likely aggregates of smaller crystallites.[15]

Figure 4 shows the resistivity ρ, Hall mobility μ, and carrier concentration n each as a function of MoO_3 content in the target. The carrier concentration in the

MZO film increases significantly from 5.3×10^{19} cm^{-3} to 2.3×10^{20} cm^{-3} as the MoO_3 content increases from 0 to 2 wt%. This suggests that an Mo atom doped in a ZnO lattice acts as an effective donor. When an Mo^{6+} ion is substituted for a Zn^{2+} ion in a ZnO lattice, four electrons are supplied as free carriers to the electric conduction of the films. However, the carrier concentration decreases to 2.3×10^{19} cm^{-3} as the MoO_3 content increases further to 5 wt%. When the MoO_3 content is higher, the number of Mo^{6+} ions in the interstitial sites increases, thus leading to a decrease in carrier concentration. A similar explanation was presented for the Zr-doped ZnO films in Ref. [16].

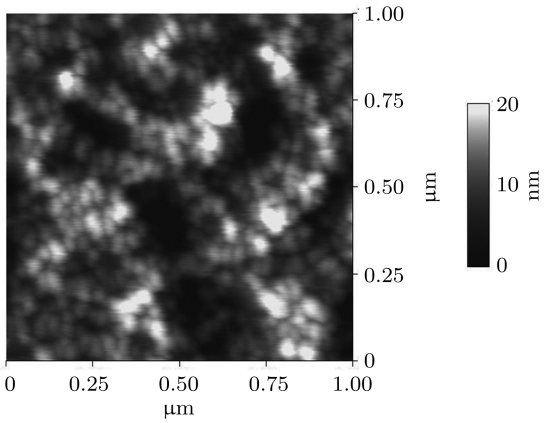


Fig. 3. AFM image (1 μm × 1 μm) of the MZO film deposited at an MoO_3 content of 2 wt%.

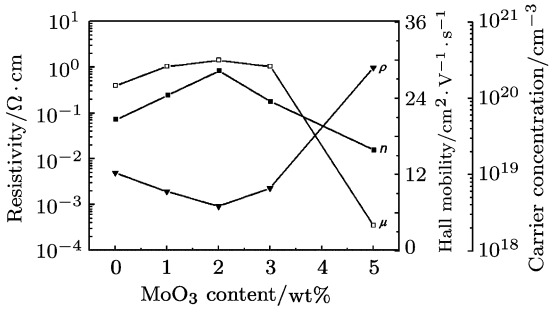


Fig. 4. Dependences of the resistivity ρ, Hall mobility μ, and carrier concentration n on the MoO_3 content for MZO films deposited at ambient temperature.

The Hall mobility increases from 26 cm$^2\cdot$V$^{-1}\cdot$s^{-1} to 30 cm$^2\cdot$V$^{-1}\cdot$s^{-1} as the MoO_3 content increases from 0 to 2 wt%. However, it shows a decrease as the MoO_3 content increases further to 5 wt%. Warmsingh *et al.*[17] reported on a similar variation of Hall mobility for Mo-doped In_2O_3 films. The carrier mobility is usually limited by several scattering mechanisms, i.e., grain boundary scattering, ionized impurity scattering, neutral impurity scattering, and scattering at other defects and dislocations.[18] In our experiments, the increase in the Hall mobility as the MoO_3 content increases to 2 wt% should be attributed to the decrease in the grain boundary scattering. As seen in Fig. 2, the crystallite size increases from 16 nm to 25 nm as the MoO_3 content increases from 0 to 2 wt%. A larger crystallite size results in a lower density of grain boundaries, which behave as barriers for carrier transport and traps for free carriers. Hence, an increase in the crystallite size can cause a decrease in grain boundary scattering.[19] The decrease in the Hall mobility as the MoO_3 content increases further to 5 wt% can be attributed to the increase in both grain boundary scattering and neutral impurity scattering. These results are consistent with the explanations of the XRD patterns.

The resistivity is proportional to the reciprocal of the carrier concentration and Hall mobility. It can be seen from Fig. 4 that the resistivity decreases from $5.0\times10^{-3}\ \Omega\cdot$cm for pure ZnO films to $9.2\times10^{-4}\ \Omega\cdot$cm as the MoO_3 content increases to 2 wt%. However, the resistivity shows a significant increase with the MoO_3 content increasing further to 5 wt%. The lowest resitivity achieved is $9.2\times10^{-4}\ \Omega\cdot$cm for the film deposited at an MoO_3 content of 2 wt% with a carrier concentration of 2.3×10^{20} cm^{-3} and a high Hall mobility of 30 cm$^2\cdot$V$^{-1}\cdot$s^{-1}.

Figure 5 shows the optical transmittances each as a function of MoO_3 content in the target. The average transmittance in the visible range shows a decrease from 91% to 80% when the MoO_3 content increases from 0 to 5 wt%, which can be ascribed to the increase in the number of scattering centres. The average

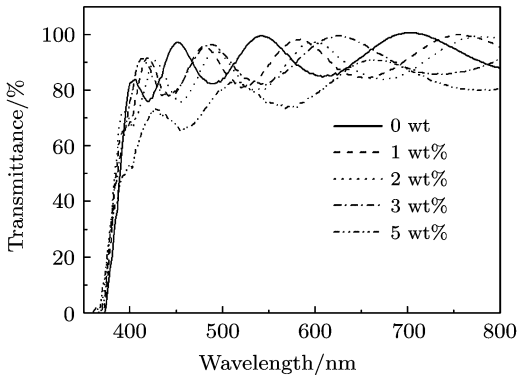


Fig. 5. Optical transmittances for MZO films with different values of MoO_3 content in the targets versus wavelength.

transmittance is calculated by averaging the value of the transmittance over a range from 400 nm to 800 nm for each sample. The absorption edge of the transmittance initially shifts to the shorter wavelength region when the MoO_3 content increases from 0 wt% to

2 wt%, which can be explained by the Burstein–Moss shift.[20] However, as MoO_3 content increases further to 5 wt%, the absorption edge shifts slightly back to a longer wavelength region. This shift can be ascribed to the increase in the number of scattering centres due to the excess in Mo content.[21]

4. Conclusion

Molybdenum-doped zinc oxide films are deposited by an RF magnetron sputtering method on glass substrates at ambient temperature. The MoO_3 content dependences of the structural, electrical, and optical properties of the films are studied. The films are polycrystalline. The lowest resistivity of the film is $9.2 \times 10^{-4}\Omega \cdot \mathrm{cm}$ with a high Hall mobility of 30 $\mathrm{cm}^2 \cdot \mathrm{V}^{-1} \cdot \mathrm{s}^{-1}$ and a carrier concentration of 2.3×10^{20} cm^{-3} at an Mo content of 2 wt%. The average transmittance in the visible region decreases from 91% to 80% with the increase in the MoO_3 content.

Acknowledgement

We thank Drs. Pang Zhi-Yong and Yang Chang-Hong for their assistance in the experiment.

References

[1] Wang Z J, Wang Z J, Li S C, Wang Z H, Lü Y M and Yuan J S 2004 *Chin. Phys.* **13** 750

[2] Gustafsson G, Cao Y, Treacy G M, Klavetter F, Colaneri N and Heeger A J 1992 *Nature* **357** 477

[3] Li L N, Chen X L, Wang F, Sun J, Zhang D K, Geng X H and Zhao Y 2011 *Acta Phys. Sin.* **60** 067304 (in Chinese)

[4] Wu C G, Shen J, Li D and Ma G H 2009 *Acta Phys. Sin.* **58** 8623 (in Chinese)

[5] Hamberg I and Granqvist C G 1986 *J. Appl. Phys.* **60** R123

[6] Kim J S, Granström M, Friend R H, Johansson N, Salaneck W R, Daik R, Feast W J and Cacialli F 1998 *J. Appl. Phys.* **84** 6859

[7] Gautier E, Lorin A, Nunzi J M, Schalchli A, Benattar J J and Vital D 1996 *Appl. Phys. Lett.* **69** 1071

[8] Ataev B M, Bagamadova A M, Mamedov V V, Omaev A K and Rabadanov M R 1999 *J. Crystal Growth* **198/199** 1222

[9] Jeong W J and Park G C 2001 *Sol. Energy Mater. Sol. Cells* **65** 37

[10] Hartnagel H L, Dawar A L, Jain A K and Jagadish C 1995 *Semiconducting Transparent Thin Films* (Bristol and Philadelphia: Institute of Physics Publishing) p. 4

[11] Shi J L, Ma H, Ma G H, Ma H L and Shen J 2008 *Appl. Phys.* A **92** 357

[12] Fang Z B, Tan Y S, Gong H X, Zhen C M, He Z W and Wang Y Y 2005 *Mater. Lett.* **59** 2611

[13] Minami T, Ida S and Miyata T 2002 *Thin Solid Films* **416** 92

[14] Klug H P and Alexander L 1974 *X-Ray Diffraction Procedures for Polycrystalline and Amorphous Materials* 2nd edn. (New York: Wiley) p. 656

[15] Altamirano-Juárez D C, Torres-Delgado G, Jiménez-Sandoval S, Jiménez-Sandoval O and Castanedo-Pérez R 2004 *Sol. Energy Mater. Sol. Cells* **82** 35

[16] Paul G K, Bandyopadhyay S, Sen S K and Sen S 2003 *Mater. Chem. Phys.* **79** 71

[17] Warmsingh C, Yoshida Y, Readey D W, Teplin C W, Perkins J D, Parilla P A, Gedvilas L M, Keyes B M and Ginley D S 2004 *J. Appl. Phys.* **97** 3831

[18] Sanon G, Rup R and Mansingh A 1990 *Thin Solid Films* **190** 287

[19] Kim H, Horwitz J S, Kushto G, Piqué A, Kafafi Z H, Gilmore C M and Chrisey D B 2000 *J. Appl. Phys.* **88** 6021

[20] Burstein E 1954 *Phys. Rev.* **93** 632

[21] Oh B Y, Jeong M C, Lee W and Myoung J M 2005 *J. Crystal Growth* **274** 453